Cement and Concrete Research 40 (2010) 502–507

Contents lists available at ScienceDirect

Cement and Concrete Research

journal homepage: http://ees.elsevier.com/CEMCON/default.asp

Concrete modelling for expertise of structures affected by alkali aggregate reaction

E. Grimal [a], A. Sellier [b], S. Multon [b,*], Y. Le Pape [c], E. Bourdarot [a]

[a] Electricité de France, Centre d'Ingénierie Hydraulique, EDF-CIH Technolac, 73373 Le Bourget du Lac Cedex, France
[b] Université de Toulouse, UPS, INSA, LMDC (Laboratoire Matériaux et Durabilité des Constructions), 135, avenue de Rangueil, F-31 077 Toulouse Cedex 04, France
[c] Electricité de France, Recherches & Développements, Dept. MMC,-avenue des Renardières-Ecuelles, F-77818 Moret-sur-Loing Cedex, France

ARTICLE INFO

Article history:
Received 16 October 2008
Accepted 10 September 2009

Keywords:
Alkali Aggregate Reaction (C)
Durability (C)
Modeling (E)
Structure Expertise

ABSTRACT

Alkali aggregate reaction (AAR) affects numerous civil engineering structures and causes irreversible expansion and cracking. In order to control the safety level and the maintenance cost of its hydraulic dams, Electricité de France (EDF) must reach better comprehension and better prediction of the expansion phenomena. For this purpose, EDF has developed a numerical model based on the finite element method in order to assess the mechanical behaviour of damaged structures. The model takes the following phenomena into account: concrete creep, the stress induced by the formation of AAR gel and the mechanical damage. A rheological model was developed to assess the coupling between the different phenomena (creep, AAR and anisotropic damage). Experimental results were used to test the model. The results show the capability of the model to predict the experimental behaviour of beams subjected to AAR. In order to obtain such prediction, it is necessary to take all the phenomena occurring in the concrete into consideration.

1. Introduction

Alkali aggregate reaction (AAR) affects numerous civil engineering structures and causes irreversible expansion and cracking. AAR is a chemical reaction between the reactive siliceous phases of aggregates and alkalis of the cement. The aggregate swelling (due to its cracking) and the product of the reaction (gel) leads to the apparition of a swelling pressure causing expansion and cracking. The consequences are a decrease in the functional capacities of civil engineering structures such as hydraulic dams. "Electricité de France" (EDF) needs better prediction of the phenomena to assess the safety level and the maintenance costs of its dams. Therefore, a numerical model integrated in a finite element computer code was developed by EDF and LMDC to calculate the behaviours of AAR-affected structures. Previous research had been carried out to develop mechanical modelling of AAR [2–7]. With the same assumption of the effect of the pressure induced by the AAR gel on the concrete considered as a porous medium, the purpose of the modelling was to add the effect of the delayed strains (creep), drying shrinkage and anisotropic damage into the constitutive laws. One of the aims is to quantify both anisotropy and amplitude of the swelling and damage due to AAR. A rheological model was thus developed to assess the coupling between the three main phenomena: creep, AAR and anisotropic damage. Recent experimental results [8–10] were simulated to check the model robustness. First, the model is presented; then the behaviours of various reinforced concrete beams damaged by AAR and stored in different moisture and loading conditions [8–10] are reproduced. Finally, results are discussed regarding the model assumptions.

2. Model description

The main developments contributed by this model concern interactions between AAR gel and long-term strain (creep) [11] on the one hand, and the swelling anisotropy induced by oriented cracking on the other hand. Particular attention is also paid to modelling the effects of moisture both on AAR and long-term strain (creep and shrinkage). In consequence, the AAR swelling depends on all these elementary phenomena. Acker [12] suggested that the basic creep of concrete was mainly due to the C–S–H behaviour (C–S–H sliding) but also to micro diffusion of water leading to consolidation phenomena. Recent experimental evidence proposed by Bernard [13] confirms this assumption. Therefore, a Visco-Elasto-Plastic (VEP) anisotropic damage model including chemical AAR pressure has been developed.

In order to model C–S–H sliding and consolidation, the model is separated into two levels:

- The first, rheological, level (VEP in Fig. 1) is based on a division of the strain and stress state in a spherical part (module VEP^s in Fig. 2(a)) and a deviatoric part (module VEP^d in Fig. 2(b)). The response of the C–S–H structure under hydrostatic stress (consolidation) is modelled by the spherical part while the deviatoric part accounts for the C–S–H sliding (without volumetric change) under shear stress.
- The second plastic level (VD^t in Fig. 1) allows large strains encountered in AAR problems to be modelled. It is linked to an anisotropic AAR traction damage model.

* Corresponding author.
E-mail address: multon@insa-toulouse.fr (S. Multon).

0008-8846/$ – see front matter © 2009 Elsevier Ltd. All rights reserved.
doi:10.1016/j.cemconres.2009.09.007

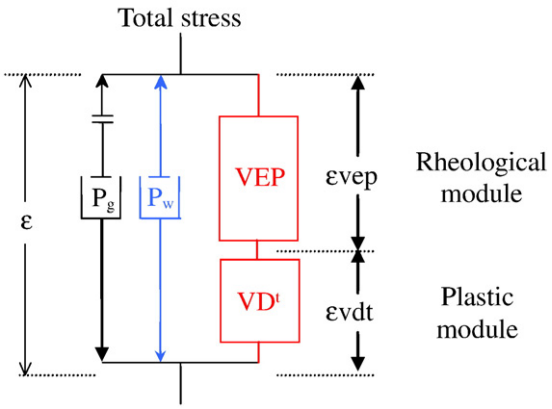

Fig. 1. Rheological model principle.

In Fig. 2, P_w is the capillarity pressure in the porosity of the concrete (deduced from a water mass balance analysis). P_g represents the AAR gel pressure. The rheological module (VEP^s and VEP^d) also contributes to tensile damage mitigation and drives realistic modelling of triaxial compressive creep. The plastic level (VD^t) allows the relaxation of self-balanced tensile stresses induced by the gel pressure around reactive aggregates.

2.1. Rheological module

The rheological model (VEP in Fig. 1) is developed in Fig. 2: (a) for the spherical part and (b) for the deviatoric part. It accounts for the multiscale porous structure of the cement paste in three levels: level '0' for the instantaneous elastic behaviour, level '1' for the long-term elastic behaviour caused by the micro-capillary porosity and level '2' for the irreversible long-term plastic behaviour caused by the modification of the C–S–H interlayer porosity [12,13]. The constitutive relations used for each module are basically the same but differences remain in the fitted coefficients used.

2.2. AAR plastic module

The plastic module (VD^t in Fig. 1) takes into account the increase of the plastic strain when the concrete is subjected to tensile stresses induced by AAR. The AAR plastic strain rate is given by Eq. (1):

$$\dot{\varepsilon}_{AAR} = \varepsilon_0 \frac{1}{(1-D_{AAR})^2} \dot{D}_{AAR} \tag{1}$$

In this phenomenological equation, ε_0 is a parameter, equal to 0.37%, determined in accordance with the experimental results given in [14], D_{AAR} is the AAR damage second order tensor. According to previous works, damage eigenvalues can be estimated with effective tensile stresses evaluated in the rheological model (Fig. 2):

$$D_{AAR} = 1 - \exp\left[-\frac{1}{m}\left(\frac{\min(\tilde{\sigma}, b_g.P_g)}{\tilde{\sigma}_u}\right)^m\right] \tag{2}$$

where $\tilde{\sigma}$ is the principal effective tensile stress governed by the Rankine criterion, $b_g.P_g$ is the gel pressure effect on the concrete skeleton (b_g is a constant parameter with the same role as the Biot coefficient in the porous mechanic theory, P_g is the gel pressure defined below), m and $\tilde{\sigma}_u$ are the parameters of the damage laws (2 parameters in compression and 2 parameters in tension). In the calculations, it is the lowest value (min) among $\tilde{\sigma}$ and $b_g.P_g$ which is taken into account. Indeed, a negative stress can avoid AAR damage increase in the direction under study (effect of compressive stresses on AAR induces strains). For example, in concrete structures with longitudinal reinforcement, it leads to anisotropic damage with cracks parallel to the reinforcement as is usually observed on real structures. This phenomenon has been clarified by mesoscopic modelling [15–19] and can be summarised using the following phenomenological relationship:

$$\sigma = (1-D) : \underbrace{(C^0 : (\varepsilon - \varepsilon_{AAR} - \varepsilon_{creep} - \varepsilon_{th}) - (b_g P_g + b_w P_w) I)}_{\tilde{\sigma}} \tag{3}$$

with σ, the apparent stress, C^0 the stiffness matrix of sound material, ε the total strain, ε_{creep} the total creep and shrinkage strains, ε_{th} the thermal strains, $b_w P_w$ the water pressure effect and $b_g P_g$ the AAR gel pressure effect. D is the anisotropic damage matrix [20,21]. In the damage matrix, each eigenvalue of damage evolves according to Eq. (4). Taking Eq. (5) into account in Eq. (3) and (4) leads to a global concrete behaviour, illustrated for a traction-compression cycle in Fig. 3.

$$D = \max(D_{AAR}, D_{mech}) \tag{4}$$

with:

$$D_{mech} = 1 - \exp\left[-\frac{1}{m}\left(\frac{\tilde{\sigma}}{\tilde{\sigma}_u}\right)^m\right] \tag{5}$$

The decrease in the stiffness and strength of the concrete is due to the largest damage among the AAR and the mechanical damage; this is taken into account by the function max() in Eq. (4).

2.3. Modelling of alkali aggregate reaction

The modelling of the AAR gel pressure is based on the assumption that there is no coupling between the mechanical stress and the

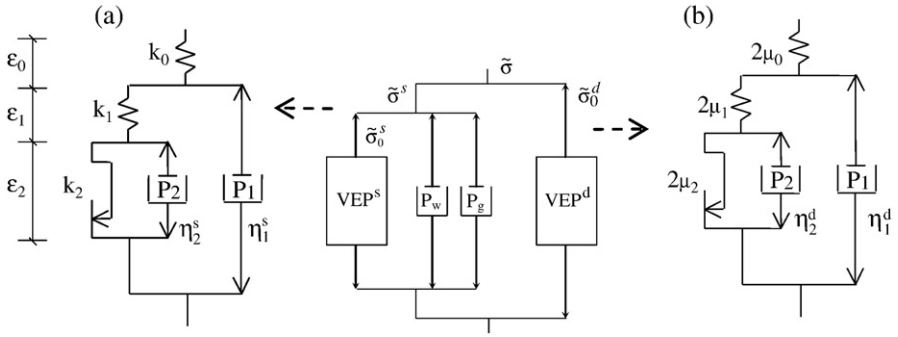

Fig. 2. (a). Spherical part of VEP module (VEP^s). C–S–H consolidation. Visco-elasto-plastic module (VEP). (b). Deviatoric part of VEP module (VEP^d). C–S–H sliding.

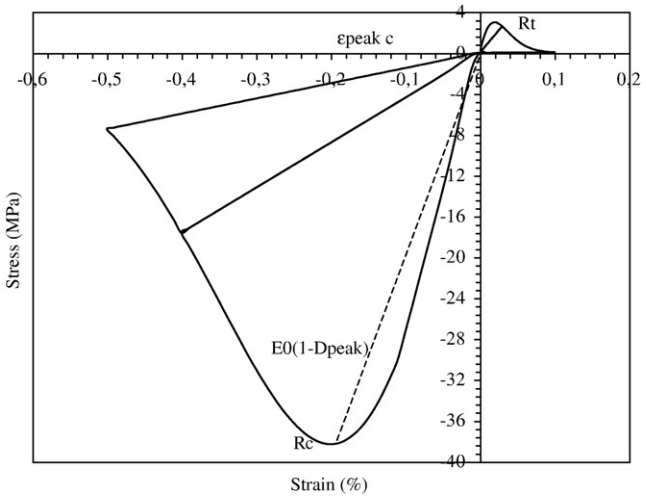

Fig. 3. Uniaxial behaviour of concrete.

chemical phenomena driving the gel formation. Eq. (6) gives P_g the swelling pressure induced by AAR:

$$P_g = M_g[AV_g - (A_0V_g + b_g tr\varepsilon^+)^+] \quad (6)$$

where M_g is an elastic modulus, V_g, the maximum volume fraction of gel created by AAR and $(\ )^+$ is the positive part of equation. A is the chemical advancement of the alkali aggregate reaction (increasing from 0, when the AAR starts, to 1 when the AAR is finished). A_0V_g is the volume of gel necessary to fill the porosity connected to the reactive aggregates and $b_g.tr\varepsilon$ is the volume of gel necessary to fill the cracks ($tr\varepsilon$ the volumetric change and b_g a coefficient to be fitted). Therefore, in this model, the pressure of the AAR gel acts only when the change of volume of aggregate due to this degradation and the gel production (AV_g) are sufficient (greater than the available porosity connected to the reactive aggregate, A_0V_g). Eq. (7) gives the chemical advancement A by a law inspired from Poyet's works [22,23]:

$$\dot{A}(Sr,t) = \alpha_0 . \exp\left[\frac{Ea}{R}\left(\frac{1}{T_{ref}} - \frac{1}{T}\right)\right] . \frac{(Sr - Sr^0)^+}{1 - Sr^0} . [Sr - A(Sr,t)] \quad (7)$$

Table 1
Model parameters.

Rheological module (Fig. 2)			
Spherical part		Deviatoric part	
k_1 (MPa)	15,000	μ_1	14,060
k_2 (MPa)	12,000	μ_2	11,250
η_1^s (MPa.d)	30,000	η_1^d (MPa.d)	112,500
η_2^s (MPa.d)	1,410,000	η_2^d (MPa.d)	1,090,800
AAR Plastic module (Eq. (5))			
Compression		Tension	
$\tilde{\sigma}_u^c$ (MPa)	39.3	$\tilde{\sigma}_u^t$ (MPa)	6.4
m^c	1.95	m^t	1.32
AAR modelling			
Pressure (Eq. (6))		Advancement (Eq. (7))	
M_g (MPa)	32,200	α_0 (day^{-1})	0.006
V_g	$0.27.10^{-2}$	E_a (J/M/°K)	47,000
b_g	0.25	S_r^0	0.20
A_0	0.09		

where α_0 is a parameter for the kinetics, E_a is the activation energy of the AAR, R the gas constant, T_{ref} is the absolute temperature of the test where α_0 is evaluated and T is the temperature in the structure. Sr and Sr^0 are the current saturation degree and the saturation degree above which the chemical reaction occurs respectively.

3. Model validation

In order to validate such models, the "Laboratoire Central des Ponts et Chaussées" (LCPC) with EDF as a partner, carried out a large experimental programme (Fig. 4). The experimental results are given in [8–10]. The behaviours of beams and specimens placed in various moisture and mechanical conditions were measured in order to investigate the combined influence of the stress state and the supply of water on swelling development. For the validation of the model, the parameters were first determined on specimens kept in various stress states [20,21] obtained during this experimental programme [8,9] (Table 1). Then, calculations were made in order to test the capability of the model to describe the behaviours of the beams of the same

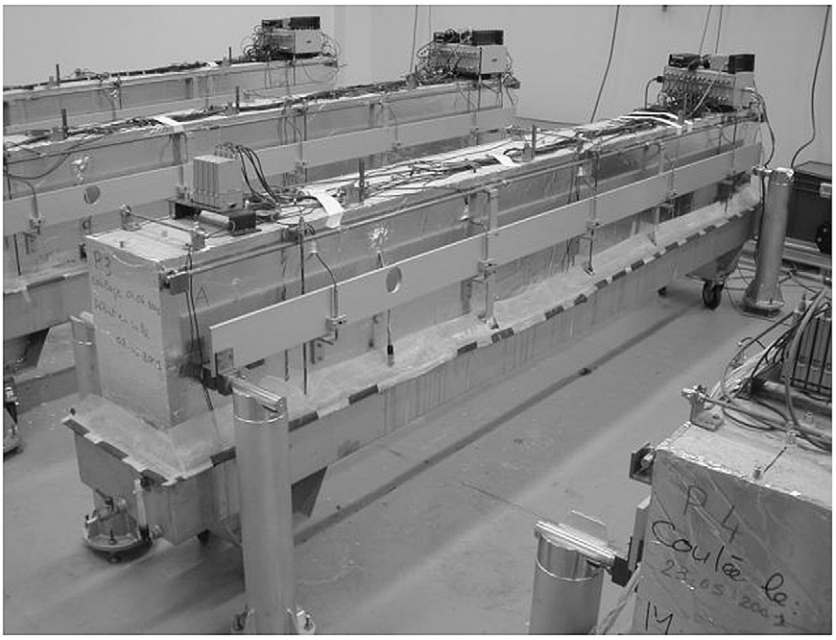

Fig. 4. Experimental beam tests [8].

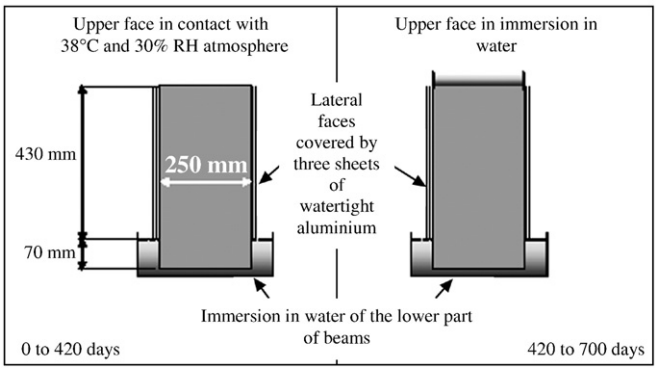

Fig. 5. Moisture controlled environment of beams.

programme [8,9]. The beams were kept for nearly 2 years in a controlled atmosphere at 38 °C and 30% RH. On their upper, lower and lateral faces, they were subjected to the moisture boundary conditions specified in Fig. 5. The lower parts were continually immerged in 70 mm of water, and the lateral faces were isolated from water. The upper faces had first been exposed to room conditions (30% RH) for 14 months (about 420 days) and were then covered by water for 9 months. A large number of moisture, strain and displacement measurements were carried out in order to describe their behaviours precisely during the test. Moreover, measurements were made of the mass variation induced by water exchanges during the different phases of the test [8,24].

3.1. Modelling of the hydrous transfer

The water concentration simulation had to be analysed with care because of the effect of water supply on AAR expansions. The moisture

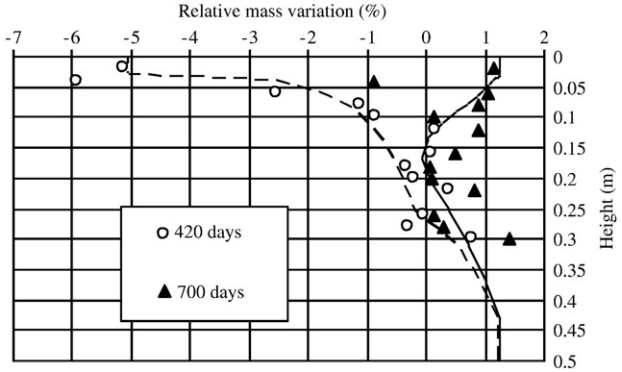

Fig. 6. Relative mass variation along the height of the beam (dotted line for simulation at 420 days and continuous line for simulation at 700 days).

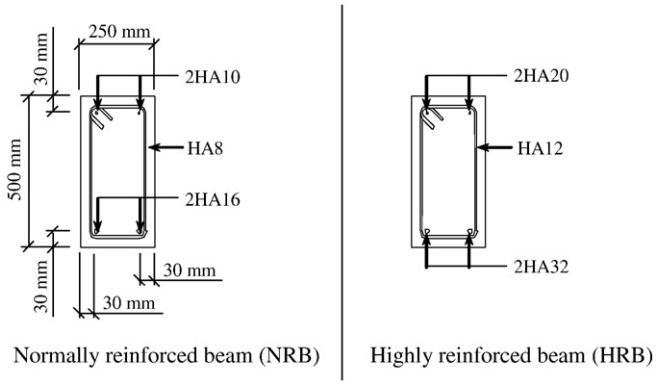

Fig. 7. Reinforcement scheme (HA = ribbed bars).

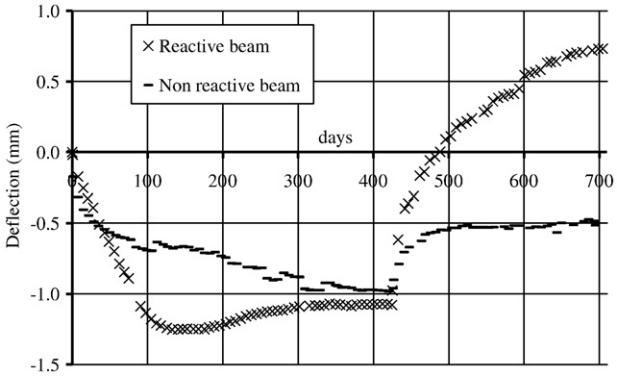

Fig. 8. Experimental mid-span deflection of the normally reinforced beam (NRB), reactive or not.

calculations of the beams were made difficult by the various boundary conditions of moisture (immerged in water in the lower part and exposed to dry air on the upper face) and the strong dependence of the moisture diffusion coefficient on the water concentration and on the moisture history of concrete (sorption or desorption). Thus, the beam was divided into two complementary parts in order to improve the water concentration simulation: the lower part was in sorption and the upper part was firstly in desorption (0–420 days) and then in sorption (420–700 days). Finally, the concrete porosity was an important parameter of the moisture calculations; it was equal to 15.8%. The moisture transfer modelling was performed according to

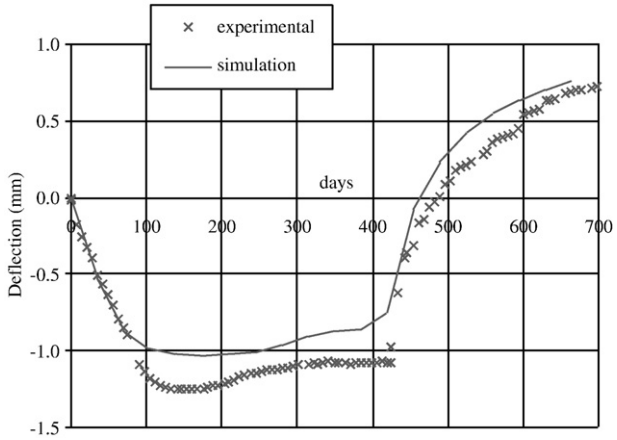

Fig. 9. Mid-span deflection of the normally reinforced beam (NRB).

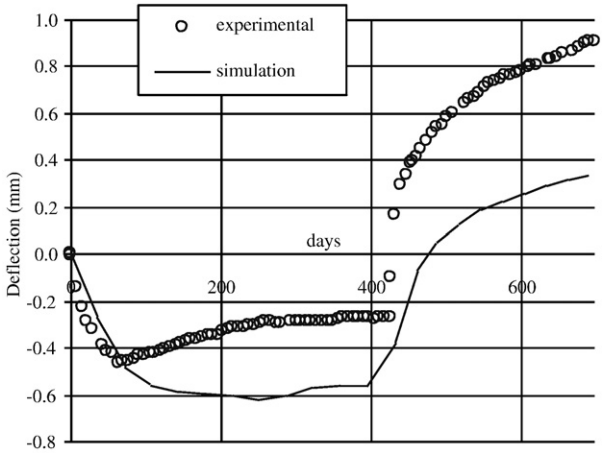

Fig. 10. Mid-span deflection of the highly reinforced beam (HRB).

the water mass balance equation (including a non-linear moisture diffusion coefficient) solved by a finite element method. Fig. 6 shows the good agreement between the calculated water concentration in terms of relative mass variations and the experimental data obtained on the reference non-reactive beam during the experimentation [8].

3.2. Modelling of the mechanical behaviour

The profile of moisture content was taken into account for each time step of the non-linear numerical procedure in order to compute the AAR advancement according to Eq. (7). Afterwards, the stress and the damage state were provided by the rheological model combined with the anisotropic damage model and the gel pressure law. The parameters of the gel pressure law and chemical advancement law (Table 1) were fitted on reactive concrete specimens in order to reproduce its behaviour under applied stresses [21]. Two beams can thus be analysed with no supplementary fitting: the first was normally reinforced (NRB) and the second was highly reinforced (HRB) (Fig. 7). The calculated deflections of the beams at mid-span are compared with the measured ones in Fig. 9 for the NRB and Fig. 10 for the HRB. The great moisture dependence of the reactive concrete is shown by the deflection history. The first part of these curves (up to about 424 days in Figs. 9 and 10) corresponds to the drying phase of the top part. In this period, the deflection was due to the development of AAR in the bottom part of the beams and, at the same time, to the shrinkage in the top part. After about 424 days, the top of the beam was covered by water. Then, the deflection reversed due to swelling caused by moisture absorption and the development of AAR in the

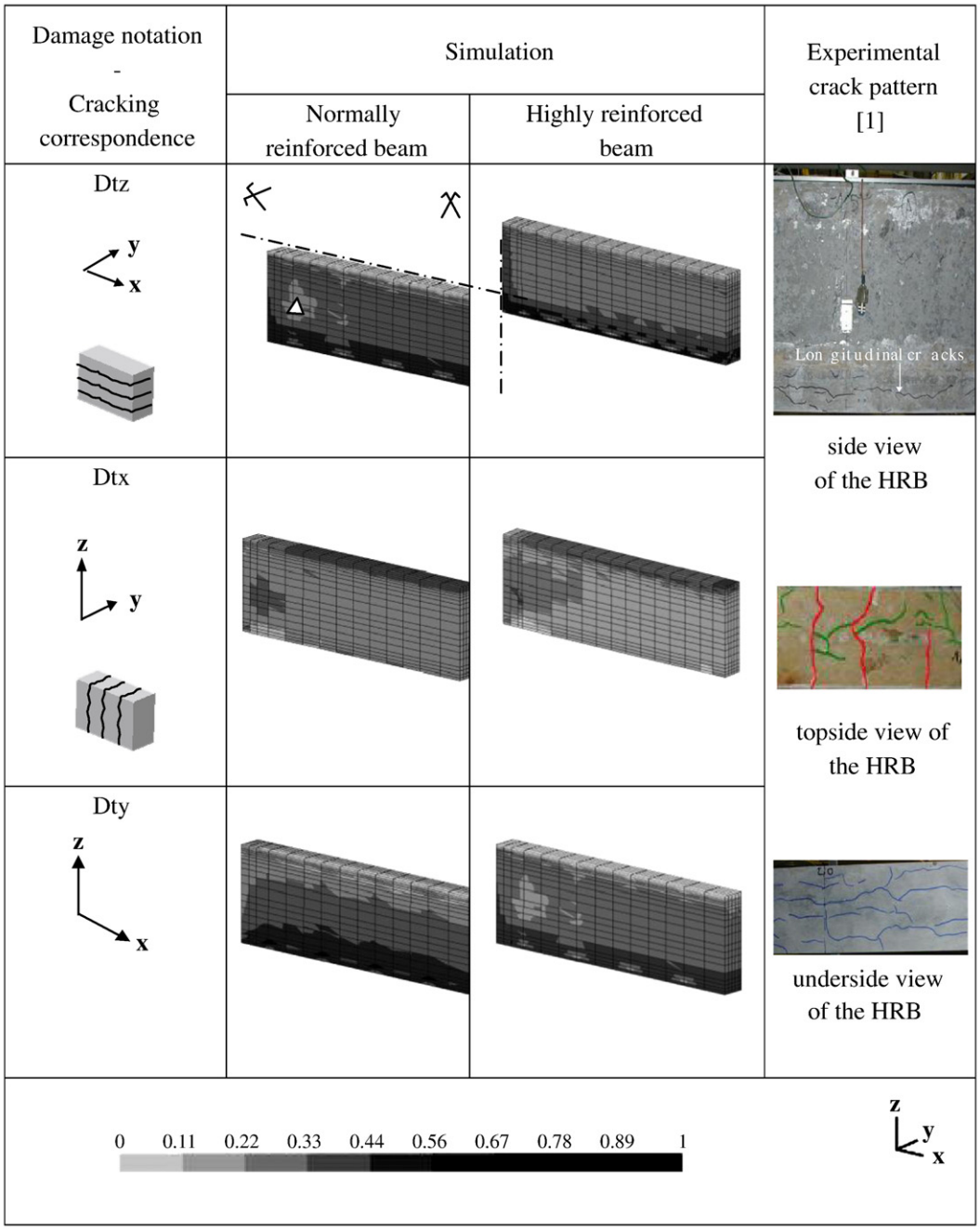

Fig. 11. Damage fields of the quarter beams (420 days) [7] (for the topside, highlighted in black: cracks appeared during drying–after 420 days, in white: cracks appeared after water was supplied [1]).

upper part of the beams. The magnitude of the deflection reversal of a non-reactive beam was small compared to the deflection reversal of a reactive beam (both normally reinforced — Fig. 8). As shown in Fig. 8, the deflection reversal of the non-reactive beam, due to water absorption, was about 0.5 mm. For the reactive beam, the deflection reversal due to water and AAR swellings was about 1.7 mm. Therefore, a large part of the deflection reversal of the reactive beam appears to be due to AAR swelling.

Both the aspect and amplitude of the curves are correctly simulated by the model (Figs. 9 and 10). The model is able to reproduce the deflection history and thus the dependence of AAR expansion on moisture. The reinforcement effect on deflection is also well reproduced. During the drying phase, the highly reinforced beam has a smaller deflection than the normally reinforced beam. In this period, AAR occurs in the bottom of the beams where reinforcement limits the longitudinal swelling and thus the deflection. The discrepancy between experiment and simulation can be partly explained by the difficulty of simulating the water concentration profiles with accuracy (Fig. 6). The prediction of the behaviour of the highly reinforced beam is not as good as the prediction performed for the normally reinforced beam. Even if the calculated deflection is not satisfactory until 200 days due to the difficulty of simulating the high non linearity in moisture transfer equation, the deflection variation during the following phase (200 days to the end) presents the same amplitude than the measurements. Moreover, previous analysis has shown that the usual ASR heterogeneity can cause such problem of precision in calculations [25]. Indeed, the anisotropy of ASR expansions is a well-known phenomenon [10,26]. It can imply differences of about 100% of ASR expansion measured on specimens cast with the same concrete and kept in the same environmental conditions. ASR-models use this type of measurement as input data and calculations. Therefore, they cannot be more precise than the input data.

The damage fields are also given by the model and can be compared to the crack patterns given in [8,10]. Fig. 11 shows the tensile damage fields 'Dtz', 'Dtx' and 'Dty' predicted for the normally and highly reinforced beams. The anisotropic cracking pattern (anisotropic damage field) obtained by calculation is in accordance with experimental observations reported in the last column of Fig. 11. Indeed, the 'Dtz' damage corresponds to the longitudinal cracks on the side of the beams. The dark zones show that the damage is more important in the lower part than in the upper as observed on the real beam (photo). The 'Dtx' damage symbolised vertical cracks on the side and transverse cracks on the top and undersides of the beams. The dark zones are in accordance with the observed cracks with large cracking on the topside and no cracking on the underside. At last, the 'Dty' damage is the longitudinal cracking. For the model, it is very important in the lower part of the beam as observed on the underside. Moreover, the highly reinforced beam shows smaller longitudinal damage (Dtx in Fig. 10) and larger transversal damage (Dty) than the normally reinforced beam. This is also in agreement with experimental observations. The larger the longitudinal rebar section is, the more the crack opening is restrained in the transversal direction, causing the gel pressure to increase until a longitudinal crack opens. This swelling transfer towards unrestrained directions highlights the anisotropic behaviour of reinforced concrete affected by AAR and justifies the necessity of using the anisotropic damage model to find the stress state in reinforced concrete structures affected by AAR.

4. Conclusion

This paper presents a model developed to calculate the mechanical behaviour of AAR-damaged structures. A model has been developed to account for all the phenomena involved in alkali aggregate reaction. In this model, the gel pressure due to AAR depending on temperature, moisture content and maximal gel volume coming from reactive siliceous parts of the aggregates. The long-term behaviour of concrete, including basic creep and shrinkage, is verified by a rheological model. Swelling transfer between restraint directions and free swelling directions is taken into consideration by the anisotropic damage model based on the effective stress concept. The model has been tested to compare the calculations with experimental results obtained on various reinforced concrete beams damaged by AAR. The comparison shows the capability of the model to reproduce the mid-span deflection and the crack pattern of the beams with acceptable accuracy. This method is part of a global methodology already used in order to predict the past and the future behaviour of a French dam affected by AAR [27]. Combined to complete study in laboratory on concrete drilled from the structures, it shows a good capability to predict the behaviour of the damaged dam. The capability of the model to predict the behaviour of real structures has thus been validated.

References

[1] A.B. Poole, A. McLachlan, D.J. Ellis, A simple staining technique for the identification of alkali–silica gel in concrete and aggregate, Cem. Conc. Res. 18 (1) (1988) 116–120.
[2] F.-J. Ulm, O. Coussy, K. Li, C. Larive, Thermo-chemo-mechanics of ASR expansion in concrete structures, ASCE, J. Eng. Mech. 126 (3) (1999) 233–242.
[3] M. Farage, J. Alves, E. Fairbairn, Macroscopic model of concrete subjected to alkali–aggregate reaction, Cem. Conc. Res. 34 (2004) 495–505.
[4] F. Bangert, D. Kuhl, G. Meschke, Chemo-hydro-mechanical modeling and numerical simulation of concrete deterioration caused by alkali–silica reaction, Int. J. Numer. Analyt. Methods Geomech. 28 (7–8) (2004) 689–714.
[5] K. Li, O. Coussy, Concrete ASR degradation: from material modeling to structure assessment, Concr. Sci. Eng. 4 (2002) 35–46.
[6] J-P. Gomes, A.L. Batista, S.B. Oliveira, Analysis of concrete dams under swelling processes, 12th Int. Conf. on AAR, Beijing, China, 2004, pp. 1148–1157.
[7] V. Saouma, R. Perotti, Constitutive model for AAR, ACI Mater. J. 103 (3) (2006) 194–202.
[8] S. Multon, 2003, "Evaluation expérimentale et théorique des effets mécaniques de l'alcali-réaction sur des structures modèles", PhD thesis, Université de Marne La Vallée, LCPC Editor, Collection Etudes Recherches LPC, Series "Ouvrages d'Art", OA 46.
[9] S. Multon, F. Toutlemonde, Effect of applied stresses on alkali–silica reaction-induced expansions, Cem. Conc. Res. 36 (2006) 912–920.
[10] S. Multon, J-F. Seignol, F. Toutlemonde, Structural behavior of concrete beams affected by alkali–silica reaction, ACI Mater. J. 102 (2) (2005) 67–76.
[11] E. Grimal, A. Sellier, Y. Le Pape, E. Bourdarot, Creep shrinkage and anisotropic damage in AAR swelling mechanism, part I: a constitutive model, ACI Mater. J. 105 (3) (2008) 227–235.
[12] P. Acker, Sur les origines du retrait et du fluage du béton, Revue Française de Génie Civil 7 (6) (2003) 761–776.
[13] O. Bernard, F.-J. Ulm, J.T. Germaine, Volume and deviator creep of calcium-leached cement-based materials, Cem. Conc. Res. 33 (2003) 1127–1136.
[14] B. Capra, A. Sellier, Orthotropic modelling of alkali–aggregate reaction in concrete structures: numerical simulations, Mech. Mat. 35 (2003) 817–830.
[15] E. Schlangen, E.J. Garboczi, Fracture simulations of concrete using lattice models: computational aspects, Eng. Fract. Mech. 57 (2/3) (1997) 319–332.
[16] E. Schlangen, K. van Breugel, Prediction of tensile strength reduction of concrete due to ASR, in: N. Banthia, et al., (Eds.), Construction Materials, The University of British Columbia, Vancouver, 2005.
[17] Cyrille Dunant, Amor Guidoum, Karen Scrivener, Micro-Mechanical Modelling of ASR, 13th ICAAR 2008 Proceedings, Broekmans & Wigum (editors), 2008, pp 632–639.
[18] Maki Mizuta, Takayuki Kojima, Kazuhiro Kuzume, Analytical evaluation of effect on ASR of RC structure using mesi-sacle concrete element by FEM, 13th ICAAR 2008 Proceedings, Broekmans & Wigum (editors), 2008 pp 994–1002.
[19] R. Naar, F. Bay, P.O. Bouchard, E. Garcia-Diaz, Modélisation couplée chimie-mécanique de la réaction alcalisilice dans le béton, 19ème Congrès Français de Mécanique Marseille, Session 14, paper n° 220, 24–28 août 2009.
[20] E. Grimal, Caractérisation des effets du gonflement provoqué par la réaction alcali-silice sur le comportement mécanique d'une structure en béton, PhD thesis, Université Paul Sabatier Toulouse, France (2007).
[21] E. Grimal, A. Sellier, Y. Le Pape, E. Bourdarot, "Creep shrinkage and anisotropic damage in AAR swelling mechanism, part II: a FEM analysis", ACI Mater. J. 105 (3) (2008) 236–242.
[22] S. Poyet, Etude de la dégradation des ouvrages en béton atteints par la réaction alcali–silice : Approche expérimentale et modélisation numérique multi-échelles des dégradations dans un environnement hydro-chemo-mécanique variable, PhD thesis, Université de Marne La Vallée, Laboratoire de mécanique, France (2003).
[23] S. Poyet, A. Sellier, B. Capra, G. Thèvenin-Foray, J-M. Torrenti, H. Tournier-Cognon, E. Bourdarot, Influence of water on alkali–silica reaction: experimental study and numerical simulations, ASCE J. Mater. Civ. Eng. 18 (4) (2006) 588–596.
[24] S. Multon, F. Toutlemonde, Water distribution in concrete beams, Mat. Struct. 37 (2004) 378–386.
[25] S. Multon, J-F. Seignol, F. Toutlemonde, Chemomechanical assessment of beams damaged by alkali–silica reaction, ASCE J. Mater. Civ. Eng. 18 (4) (2006) 500–509.
[26] C. Larive, M. Joly, O. Coussy, Heterogeneity and anisotropy in ASR-affected concrete: consequences for structural assessment, Proc., 11th Int. Conf. on AAR, Centre de Recherche Interuniversitaire sur le Béton, Québec, Canada, 2000, pp. 969–978.
[27] A. Sellier, E. Bourdarot, S. Multon, M. Cyr, E. Grimal, Combination of structural monitoring and laboratory tests for the assessment of AAR-swelling — application to a gate structure dam, ACI Mater. J. 106 (3) (2009) 281–290.